Water Research 254 (2024) 121441

Contents lists available at ScienceDirect

Water Research

journal homepage: www.elsevier.com/locate/watres

Why is HSO_5^- so effective against bacteria? Insights into the mechanisms of *Escherichia coli* disinfection by unactivated peroxymonosulfate

Na Tian [a,b,*], Luciana Carina Schmidt [c], María Jesús Abeledo Lameiro [d,e], María Inmaculada Polo-López [d,e], María Luisa Marín [c], Francisco Boscá [c], Isabel del Castillo González [b], Aurelio Hernández Lehmann [b], Stefanos Giannakis [b,*]

[a] School of Chemistry and Chemical Engineering, Hunan University of Science and Technology, Xiangtan 411201, PR China
[b] Universidad Politécnica de Madrid, E.T.S. de Ingenieros de Caminos, Canales y Puertos, Departamento de Ingeniería Civil: Hidráulica, Energía y Medio Ambiente, Unidad docente Ingeniería Sanitaria, c/ Profesor Aranguren, s/n, ES-28040, Madrid, Spain
[c] Instituto de Tecnología Química, Universitat Politècnica de València-Consejo Superior de Investigaciones Científicas, Avenida de los Naranjos s/n, Valencia 46022, Spain
[d] CIEMAT-Plataforma Solar de Almería, Ctra. Senés km 4, Almería 04200, Spain
[e] Solar Energy Research Centre (CIESOL), Joint Centre University of Almería-CIEMAT, Carretera de Sacramento s/n, Almería E-04120, Spain

ARTICLE INFO

Keywords:
Gram-negative bacteria
Peroxymonosulfate
Gene knock-out mutants
Radical pathway
Cell death

ABSTRACT

This study examined the antimicrobial efficacy of peroxymonosulfate (PMS) against bacteria, using *Escherichia coli* (*E. coli*) as a model organism. Our investigation delineates the complex mechanisms exerted by unactivated PMS. Thus, an initial redox reaction between PMS and the target biomolecules of bacteria generates $SO_4^{\bullet-}$ as the pivotal reactive species for bacterial inactivation; to a lesser extent, •OH, $^1O_2$, or $O_2^{\bullet-}$ may also participate. Damage generated during oxidation was identified using an array of biochemical techniques. Specifically, redox processes are promoted by PMS and $SO_4^{\bullet-}$ targets and disrupt various components of bacterial cells, predominantly causing extracellular damage as well as intracellular lesions. Among these, external events are the key to cell death. Finally, by employing gene knockout mutants, we uncovered the role of specific gene responses in the intracellular damage induced by radical pathways. The findings of this study not only expand the understanding of PMS-mediated bacterial inactivation but also explain the ten-fold higher effectiveness of PMS than that reported for H_2O_2. Hence, we provide clear evidence that unactivated PMS solutions generate $SO_4^{\bullet-}$ in the presence of bacteria, and consequently, should be considered an effective disinfection method.

1. Introduction

In recent years, the number of waterborne diseases caused by pathogenic microorganisms has increased, posing a significant threat to human health (Ramirez-Castillo et al., 2015; WHO, 2017). Treated and safe drinking water can reduce the burden on water resources and guarantee human health; hence, effective inactivation of pathogenic microorganisms in water continues to be an important research topic. Water disinfection is an essential step in treatment facilities to kill or inactivate pathogenic microorganisms (Gelover et al., 2006; Lanrewaju et al., 2022). Conventional disinfection methods include ultraviolet (UV), chlorine, and ozone disinfection, *etc.* (Cho et al., 2010; Choi et al., 2021; McGuigan et al., 2012). Although these disinfection techniques have been employed for many years, they have some serious deficiencies and limitations, including low efficiency, high energy consumption, incomplete inactivation, and the production of carcinogenic disinfection by-products (DBPs) (Simpson and Hayes, 1998; Von Gunten et al., 2001). Therefore, the development of highly efficient disinfection technologies is required to reduce waterborne pathogens that can be detrimental to public health.

Over the last few decades, advanced oxidation processes (AOPs) have emerged as efficient and promising technologies for mineralizing refractory organic contaminants and inactivating pathogens (Giannakis et al., 2016; Jiménez et al., 2020). Specifically, AOPs generate various reactive oxygen species (ROS) with high oxidation capabilities, including hydroxyl radicals (•OH), sulfate radicals ($SO_4^{\bullet-}$), superoxide radicals ($O_2^{\bullet-}$), hydrogen peroxide (H_2O_2), ozone (O_3), and singlet oxygen ($^1O_2$) (Giannakis, 2019; Karbasi et al., 2020; Rodríguez-Chueca

* Corresponding authors.
E-mail addresses: tianna@hnust.edu.cn (N. Tian), stefanos.giannakis@upm.es (S. Giannakis).

https://doi.org/10.1016/j.watres.2024.121441
Received 2 December 2023; Received in revised form 5 March 2024; Accepted 7 March 2024
Available online 8 March 2024
0043-1354/© 2024 The Authors. Published by Elsevier Ltd. This is an open access article under the CC BY license (http://creativecommons.org/licenses/by/4.0/).

et al., 2019). During disinfection, these species can attack the structures and components of cells, causing cell death via extracellular and intracellular damage. The cell envelope (both the cell wall and membrane), enzymes, and intracellular components (DNA and RNA) of pathogenic microorganisms have been identified as targets of ROS (Dutta et al., 2019; Xiao et al., 2019), all of which contribute to cell death.

Among AOPs, persulfate-based ones have attracted interest as highly efficient oxidation technologies because they use reagents that are more stable, cheap, non-toxic, and safer than those employing H_2O_2 and O_3 (Luo et al., 2021; Mohammadi et al., 2021). As reported, the photolytic and/or catalytic activation of PMS is effective for bacterial inactivation, including PMS/UV or UV-A LED (Berruti et al., 2021a; Qi et al., 2020; Yao et al., 2022), PMS/solar radiation (Berruti et al., 2023, 2021b), PMS/transition metal/UV-A LED (Rodríguez-Chueca et al., 2017), PMS/Fe(VI)/solar light (López-Vinent et al., 2022), Cu(II)/PMS/Cl^- (Lee et al., 2020), and $CoFe_2O_4$/PMS (Rodríguez-Chueca et al., 2020). One of the first reports on the inactivation of various microorganisms in simulated and real winery wastewater by different persulfate-based oxidation processes indicated that the inactivation efficiency and rate of bacteria markedly increased through the photolytic and catalytic activation of PMS compared with PMS alone (Rodríguez-Chueca et al., 2017). According to the investigation of the inactivation mechanism, several works demonstrated that •OH and $SO_4^{\bullet-}$ played important roles and •OH was the dominant reactive species in bacterial inactivation (Amiri et al., 2021; López-Vinent et al., 2022). Nevertheless, non-radical species in the $^1O_2$-dominated process for bacterial inactivation have also been suggested, in which $^1O_2$ generated from PMS decomposition first attacks the bacterial cell membranes and then enters the cell and upregulates intracellular reactive species, further causing cell membrane damage and DNA degradation, ultimately leading to irreversible cell inactivation (Jiang et al., 2022).

Although previous studies have been devoted to the investigated water disinfection by sulfate radical-based AOPs, their disinfection efficiency is always a major concern, and the possible inactivation pathways of bacteria by PMS are not well elucidated. For instance, the versatile roles of ROS generated from the PMS oxidation process in bacterial inactivation have been less discussed, and an analogy from H_2O_2 has been proposed to explain its action (Feng et al., 2020; Giannakis et al., 2018). Moreover, most studies have focused on complex PMS activation methods for bacterial disinfection and there have been almost no studies on the mechanisms of bacterial death by PMS alone (Amiri et al., 2021; López-Vinent et al., 2022). This is logical because there is an obvious synergy between PMS and its activation methods, and the alternative coupling of PMS with light/metal ions/heterogeneous catalysts significantly affects sterilization efficiency and pathways. However, elucidating the action of pristine PMS in disinfection processes is yet to be addressed, and is key to the further application of activated PMS. It is worth mentioning that, the study carried out by Berruti et al. (Berruti et al., 2022), where the reactivity of $SO_4^{\bullet-}$ against cell-wall compounds commonly found in gram-negative and gram-positive bacteria was investigated for the first time using the laser flash photolysis (LFP) technique. These results evidenced that $SO_4^{\bullet-}$ reacts with common cell-wall components through the H-abstraction mechanism ($kSO_4^{\bullet-} < 10^8\ M^{-1}\ s^{-1}$), while a mechanism based on electron transfer reaction was observed specifically for the aromatic amino acids (AAA) only present in porins of the gram-negative outer membrane (commonly less resistant to oxidative processes than gram-positive ones).

In this study, *E. coli* was chosen as the target microorganism to dissociate the PMS-induced inactivation pathways and unravel its fundamental aspects. First, the inactivation performance of *E. coli* by PMS was evaluated and compared with that of other inorganic peroxides (such as peroxydisulfate (PDS) and H_2O_2). The postulated mechanism of action of PMS is based on disinfection and PMS consumption kinetics as well as the quantification and localization of the damage. In addition, the involvement of ROS in the PMS oxidation process is comprehensively discussed to elucidate the role of diverse reactive species. Moreover, this study was complemented by investigating the action of the major reactive species using knockout mutants, thereby offering a holistic and integrated explanation of the high efficacy of PMS against bacteria.

2. Materials and methods

2.1. Chemicals and reagents

The chemicals and reagents used in this study are listed in Text S1 (Supplementary Information, SI). Wild-type *E. coli* K12 environmental isolate strain, (parent) *E. coli* (MG 1655), and its derivative knockout strains were used in this study. Details of the bacterial strains are listed in Text S2 of the SI.

2.2. Experimental procedure for bacterial inactivation tests

At the beginning of each test, all supplies, including the materials, solutions, and reactors, were autoclaved. To perform the experiments, cylindrical Pyrex glass reactors (50 mL) were used, and *E. coli* was firstly suspended into sterilized water. Then, a PMS solution of a certain concentration was added to a suitable aliquot of the *E. coli* suspension under constant stirring (450 rpm) at 25 °C. Samples were collected at different time intervals and $Na_2S_2O_3$ (0.1 M) was immediately added to terminate the disinfection reaction. Then, the bacterial concentration in the samples was determined, as indicated in Text S2. After each experiment, the reactors were washed with demineralized water and sterilized.

2.3. Biochemical analytical techniques for determination of bacterial inactivation mechanisms

2.3.1. Determination of lipid peroxidation

Malondialdehyde (MDA), the main oxidation product of lipid peroxidation, is generally used to evaluate the oxidation of bacterial membranes by reacting with thiobarbituric acid (TBA-1) (Zeb and Ullah, 2016). The standard MDA solution (1 mL, 1 mM) was placed in a 10 mL test tube and mixed with TBA-1 (1 mL, 4.0 mM). The mixture was then heated in a boiling water bath at 95 °C for 60 min. After cooling to room temperature, the absorbance of the solution was measured at 532 nm by using a UV–visible spectrophotometer (Shimadzu, Japan). Each sample was repeated three times, according to the above procedure. The blank sample was repeated ($n = 3$) by replacing the standard or sample (10^8 CFU/mL) with water.

2.3.2. Membrane permeability and damage

Ortho-nitrophenyl-β-D-galactoside (ONPG) is usually regarded as a permeability probe that can react with the intracellular enzyme (β-D-galactosidase) in *E. coli* by hydrolysis to produce a chromogenic substrate (Huang et al., 2000). Hydrolysis of ONPG by intact whole cells was determined using this method. The hydrolysis kinetics were determined spectrophotometrically by measuring the absorbance at 420 nm. Details of the analytical technique are presented in Text S3.

2.3.3. Protein content

Cell protein content was determined using the Bradford method as previously described (Giannakis et al., 2022). To quantify the protein concentration in (total) cell lysates (10^8 CFU/mL), albumin from chicken eggs was used as the standard. The standard was diluted to final concentrations of 0, 2.5, 5, 7.5, 10, and 12.5 μg/mL in 0.5 mL of 50 mM Tris-buffered saline (pH 8.0). For the standard and the protein samples, 0.5 mL of Coomassie blue stain was added to the standard and protein samples, and absorbance was measured at OD_{595} after 10 min. Analyses were performed at an initial bacterial concentration of 10^8 CFU/mL.

2.3.4. Cell proliferation and viability assay

Cell proliferation was examined using a simplified version of the 2, 3-bis(2-methoxy-4-nitro-5-sulfophenyl)−2H-tetrazolium-5-carboxanilide (XTT) assay at 10^8 CFU/mL. First, 50 μL of XTT (1 mg/mL) and 150 μL of the sample (exposed to 30 mg/L PMS) were added to a 96-well plate and subsequently incubated at 37 °C for 5 h. After incubation, the reduction in the percentage of viable cells was determined by measuring absorbance at a wavelength of 495 nm using a microplate reader (Multiskan SkyHigh; Fisher Scientific). The inhibition rate (%) of XTT was calculated using Eq. 1:

$$\text{Inhibition rate}(\%) = [(A_0 - A_t) / A_0] \times 100\% \quad (1)$$

where A_0 and A_t are the measured absorbance at 495 nm at time 0 and time t, respectively.

2.3.5. Extraction and quantification of DNA

To investigate DNA damage by PMS (30 and 50 mg/L), the 16S rRNA gene was analyzed as a model. The 16S rRNA gene is conserved in all microorganisms and consists of seven genes in *E. coli* (Ellwood M and M, 1982). The extraction and quantification of DNA in this study were performed as described in Text S4.

2.4. Analytical chemical techniques for characterization of the disinfection tests and mechanisms

As depicted in Text S5, the residual PMS concentration was determined, and some samples were analyzed by ultra-performance liquid chromatography (UPLC) using an ACQUITY UPLC system (Waters, Milford, MA, USA). Proton nuclear magnetic resonance (NMR) spectra were recorded on a Bruker AVANCE spectrometer (^{1}H NMR at 400 MHz) in D_2O. The Mnova software (Mestrelab Research) was used for spectral processing. Electron paramagnetic resonance (EPR) and ROS trapping experiments were performed and are shown in Text S6 to detect the reactive species during disinfection.

3. Results and discussion

3.1. Disinfection efficacy of commonly employed oxidants: which inorganic peroxide damages bacteria the most?

As shown in Fig. 1a, there was no obvious decline in *E. coli* inactivation under both 0.1 mM H_2O_2 and PDS, indicating that H_2O_2 and PDS cannot kill the cells effectively at this concentration. Meanwhile, 10^6 CFU/mL *E. coli* was inactivated within 75 min by PMS oxidation at the same molar concentration, suggesting that PMS alone is capable of disinfecting *E. coli*. Higher concentrations of H_2O_2 and PDS may lead to disinfection (Bianco et al., 2017), but from the results depicted in Fig. 1a, the disinfection efficiency of PMS towards *E. coli* is superior to that of H_2O_2 and PDS at the concentrations used in our study, chosen in a way that allows easy monitoring of kinetics.

E. coli inactivation efficiency increased with increasing PMS concentration, and most of the PMS remained in the solution after disinfection (Fig. 1b). More specifically, 5 mg/L PMS had minimal effect on the inactivation efficiency of *E. coli* (less than 1 logU), while 1.02×10^5 CFU/mL *E. coli* and 6.07 mg/L residual PMS were still observed in the experiments performed with 10 mg/L PMS after 120 min of treatment. Approximately 4.44 log *E. coli* reduction and 5.72 mg/L residual PMS concentration were measured after 120 min at 15 mg/L PMS. Moreover,

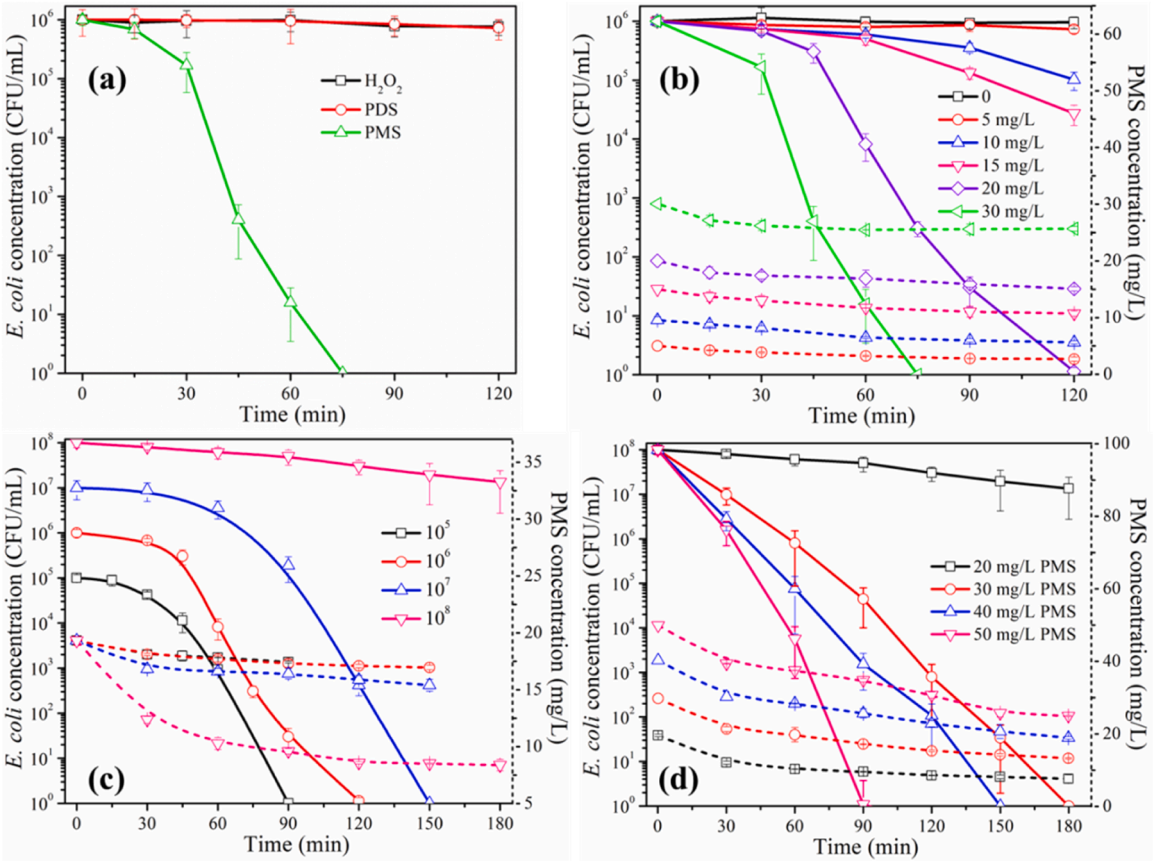

Fig. 1. (a) *E. coli* inactivation using different oxidants (at equimolar concentrations) under the same conditions. The experimental conditions were as follows: [*E. coli*] = 10^6 CFU/mL (optical density (OD_{600}) = 0.005), $[Oxidant]_0$ = 0.1 mM. Influence of PMS concentration on *E. coli* inactivation and residual PMS at (b) 10^6 CFU/mL and (d) 10^8 CFU/mL of initial *E. coli* concentration (OD_{600} = 0.005 and 0.05). (c) Viability curve of *E. coli* under unactivated PMS treatment and residual PMS at different initial *E. coli* concentrations at 20 mg/L PMS. (The solid and dotted lines represent the *E. coli* and PMS concentration curves, respectively.).

a notable improvement in inactivation efficiency was observed with 20 mg/L PMS, and 6-logU bacteria were inactivated within 120 min. Similarly, inactivation of 6-logU *E. coli* was observed with 30 mg/L PMS after 75 min of treatment, and approximately 4.79 mg/L of PMS was reduced during this oxidation process. These results indicate that increasing the oxidant dosage can enhance the generation of reactive oxygen species during disinfection, which further results in higher inactivation efficiency of *E. coli*.

Because of the 6-logU inactivation of *E. coli* within 120 min, 20 mg/L PMS was chosen for subsequent tests to investigate the influence of the initial *E. coli* concentration. As shown in Fig. 1c, the inactivation of 10^6 CFU/mL *E. coli* was achieved within 90 min when the bacterial concentration decreased to 10^5 CFU/mL. A longer contact time was required to kill all the bacteria at a higher initial concentration. While still 7.13 log *E. coli* survived at an initial concentration of 10^8 CFU/mL even in 180 min, and 12.09 mg/L PMS was consumed in this disinfection process, suggesting this dosage of PMS was inadequate to inactivate 6-logU *E. coli* within the set timeframe. Hence, a higher PMS dosage was used to better explore the disinfection performance at a high initial concentration of *E. coli*, and a higher inactivation efficiency was achieved, as shown in Fig. 1d. It has been reported that PMS with a strong oxidation potential (1.8 V) (Wang and Wang, 2018) can damage the bacterial membrane (0.7 eV) (Brasca et al., 2007; Oktyabrskii and Smirnova, 2012) and directly oxidize cells. When the initial PMS concentration was increased from 30 to 50 mg/L, 6-logU removal was achieved from 180 to 90 min, and the consumption of PMS was 16.52, 21.37, and 24.97 mg/L, respectively.

3.2. What is the primary mode of PMS action? Assessment of E. coli inactivation kinetics

Based on the experimental data, the disinfection process can be adequately fitted by a well-established Shoulder and Log-Linear model using GInaFiT Microsoft Excel Add-in (Geeraerd et al., 2005). The detailed equation for this model is as follows:

$$N = N_0 \times e^{(k\times t)}_{max} \times \left(e^{(-k\times SL)}_{max}\right) / \left(1 + \left(e^{(-k\times SL)}_{max} - 1\right) \times e^{(-k\times t)}_{max}\right) \quad (2)$$

where N is the number of cultivable bacteria at time t, N_0 is the initial number of bacteria at time 0, k_{max} is the slope of the regression (min^{-1}), t is the time (min), and SL is the lag phase (shoulder length, min).

The results fitted by the SL&log-linear decay models are summarized in Fig. 2a and Table S2. The increase in the initial PMS concentration exhibited an almost linear effect on the inactivation rate and the lag phase. For instance, the apparent first-order kinetic rate improved from 0.0021 to 0.2620 min^{-1} when the PMS concentration increased from 5 to 30 mg/L at an *E. coli* concentration of 10^6 CFU/mL, which was superior to the rate constants under PMS alone and PMS-combined light treatments in Table S3 of the SI. Similarly, the kinetic rate increased from 0.0120 to 0.1810 min^{-1} with an increase in PMS concentration from 20 to 50 mg/L at an *E. coli* concentration of 10^8 CFU/mL. Hence, it can be concluded that PMS dosage is a significant factor in the inactivation of *E. coli*, and that their inactivation at lethal concentrations follows first-order kinetics after an initial lag phase.

This behavior might be an indicator of the disinfection action mode itself; the initial delay means that either bacteria have defense mechanisms that allow them to cope with the oxidative damage caused by PMS or that there is a threshold of damage that needs to be reached before bacteria become inactivated. To assess this, the viability of *E. coli* was evaluated using the XTT assay, and it declined to 47.83 % after treatment with unactivated PMS for 180 min (Fig. 2b), which might be influenced by the existence of bulk reductants reacting with XTT. In any case, this is the first firm indication of a prevalent extracellular pathway.

3.3. Where does PMS act? Estimation of cell wall damage and membrane permeability

To evaluate the possibility of primary PMS attacks on the bacterial cell wall, and therefore the localization of cell damage, malondialdehyde (MDA) generation and ortho-nitrophenyl-β-D-galactoside (ONPG) hydrolysis rate were assessed during the PMS disinfection process. Solar/TiO_2 tests were performed in parallel to compare PMS with the known extracellular action of photocatalysis (Ruales-Lonfat et al., 2014). There was no obvious MDA release in *E. coli* alone (Fig. 3a), which was consistent with the inactivation efficiency without PMS treatment. A significant increase in MDA concentration and similar trends in MDA formation were observed for both 30 and 50 mg/L PMS treatments. This result indicated that external attacks on cell walls by PMS occurred, and the peroxidation of unsaturated lipids in bacterial membranes arose by the PMS oxidation process, which led to an increase in membrane permeability (even membrane disruption) and ultimately bacterial death. However, it is interesting to note that the concentration of MDA accumulated in the 30 mg/L PMS treatment was higher than that in the 50 mg/L PMS treatment. This apparent contradiction can be explained by the reactivity of MDA with PMS (Fig. S2). Because TiO_2 mainly acts in the extracellular domain during photocatalysis, it can be suggested that bacterial inactivation by PMS is not only an extracellular action, but may also take place intracellularly.

Peaks with identical shapes were observed for both PMS oxidation and TiO_2 photocatalysis (Fig. 3b), and the hydrolytic rates of ONPG increased immediately, reaching their maximum at 30 min. Interestingly, the most rapid hydrolysis of ONPG occurred during TiO_2

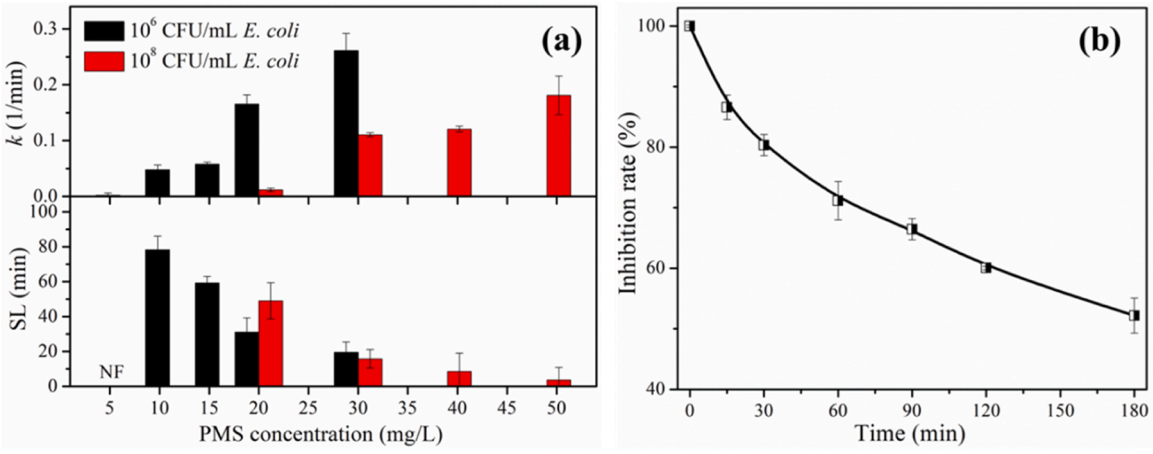

Fig. 2. (a) Disinfection kinetics and the corresponding shoulder length (SL) fitted by shoulder and log-linear models under different concentrations of PMS and *E. coli*. (b) Estimation of the inhibition rate of viable *E. coli* cells under unactivated PMS treatment using the XTT assay. NF: not found.

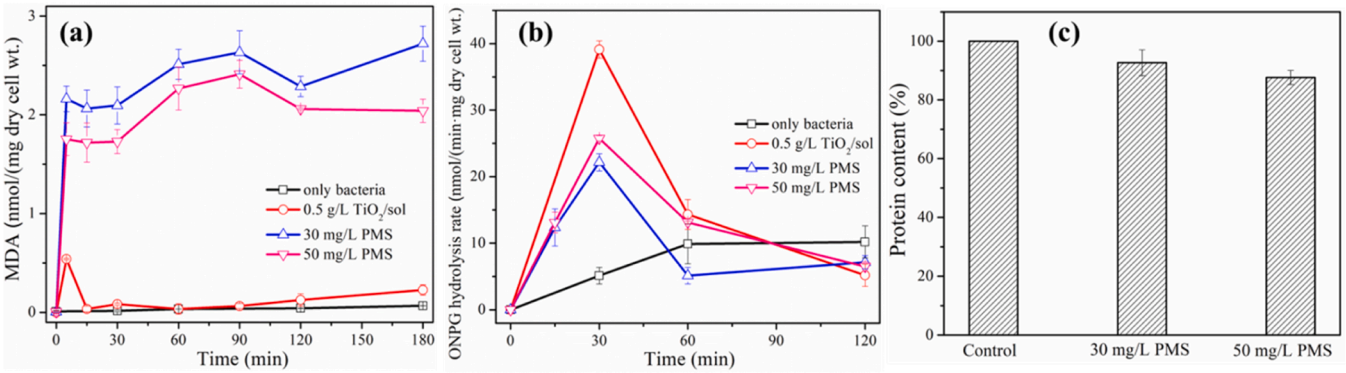

Fig. 3. (a) Malondialdehyde (MDA) released from lipid peroxidation, (b) evolution of ortho-nitrophenyl-β-D-galactoside (ONPG) formation during *E. coli* inactivation in different oxidation systems, and (c) total protein content after 120 min of unactivated PMS treatment (control: only bacteria). The experiments were performed using an initial bacterial concentration of 10^8 CFU/mL (OD_{600}=0.5).

photocatalysis compared to PMS oxidation, which was distinctly different from the MDA results. This result proved that bacterial inactivation mediated by TiO_2 photocatalysis and PMS oxidation could be attributed to damage to the cell envelope and enhancement of membrane permeability, possibly even causing the diffusion and entry of molecules into cells during PMS treatment, and ultimately, *E. coli* inactivation. The protein concentration decreased during PMS treatment (Fig. 3c), indicating that the protein was degraded by reactive species produced during PMS inactivation. In the 30 mg/L and 50 mg/L PMS treatments (120 min), the total protein content of the cell lysate was reduced by 7.34 % and 12.37 %, respectively. This indicates that the damage to the membrane was the result of an oxidative process. Meanwhile, the intracellular protein oxidation may also occur because of enhanced cell wall permeability.

Based on the collective results of MDA, ONPG, and protein measurements, the following scenarios are plausible: first, an external attack is validated, followed by an increase in cell wall permeability (less protein and more lipid oxidation). Hence, the reactive species that participate in the degradation process and whether intracellular inactivation occurs (or to what extent) remain to be determined.

3.4. What is the primary ROS involved in PMS disinfection? Scavenger and EPR tests

3.4.1. Scavenger experiments

Based on the findings in previous sections, *E. coli* inactivation mediated by PMS oxidation could be attributed to extracellular and intracellular damage. Hence, studies on the mechanisms of inactivation pathways have been conducted by analyzing the transient species involved in PMS disinfection, including radical and non-radical species. As shown in Fig. 4a, the inactivation time of *E. coli* was prolonged to 120 and 90 min in the presence of MeOH and TBA, respectively. Interestingly, greater inhibition of *E. coli* inactivation was observed in PMS systems with the addition of MeOH than in the presence of the same amount of TBA, which clearly shows that $SO_4^{\bullet-}$ participates more than •OH in *E. coli* inactivation.

To gain insights into the potential involvement of $^1O_2$ in PMS disinfection, *E. coli* inactivation was evaluated in an aqueous 50 % D_2O solution to increase the lifetime of $^1O_2$ (Kohantorabi et al., 2019). Faster bacterial inactivation was observed in 50 % D_2O than in H_2O, suggesting the generation and reactivity of $^1O_2$ during disinfection. However, changes in the diffusion rate constant of bacteria and/or PMS in D_2O cannot be disregarded. SOD, a well-known antioxidant enzyme that catalyzes the dismutation of superoxide radicals ($O_2^{\bullet-}$) into H_2O_2 and O_2, has been used as an $O_2^{\bullet-}$scavenger (Chen et al., 2021; Sawyer and Valentine, 1981). The low inhibition of *E. coli* inactivation efficiency observed when SOD was added to the disinfection process revealed that the possible involvement of $O_2^{\bullet-}$ is not significant if we consider that SOD is also an organic material that can be oxidized by $SO_4^{\bullet-}$ and •OH. Based on these results, $SO_4^{\bullet-}$ is suggested to be the primary species involved in *E. coli* inactivation, followed by •OH, $^1O_2$, and $O_2^{\bullet-}$.

The effect of dissolved oxygen on *E. coli* inactivation was tested to assess the validity of the suggested pathways. The results shown in Fig. 4b confirm that $^1O_2$ and $O_2^{\bullet-}$ are not the dominant reactive species

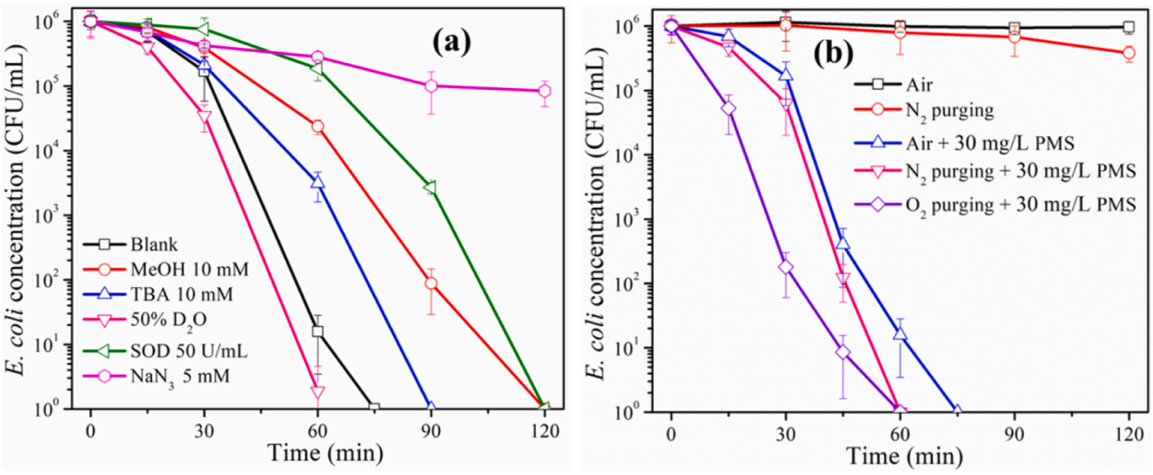

Fig. 4. E. coli inactivation curves by unactivated PMS (a) with different scavengers and (b) under different atmospheres. Experimental conditions: [*E. coli*] = 10^6 CFU/mL (OD_{600}=0.005) and $[PMS]_0$ = 30 mg/L.

generated during PMS disinfection in the aerated medium because a similar result was obtained when the sample was purged with N_2. In this context, the improved inactivation efficiency of *E. coli* by saturation of dissolved oxygen (42.12 mg/L) in the reaction solution could be attributed to an increase in the lipid peroxidation of cell membranes, which proceeds via a free-radical mediated chain reaction, and because oxygen is required for its propagation, it accelerates when more oxygen is present in the medium.

3.4.2. EPR measurements

In PMS oxidation for contaminant degradation, electron transfer is usually considered to be the dominant contributor to the generation of reactive radicals, including $^{\bullet}OH$, $SO_4^{\bullet-}$, $^1O_2$, and $O_2^{\bullet-}$ (Yan et al., 2018). To further confirm the reactive species involved in bacterial inactivation in PMS aqueous medium, several trapping experiments were performed, and the results are presented in Fig. 5. According to an EPR study, unactivated PMS oxidizes 5,5-dimethyl-1-pyrrolidine N-oxide (DMPO). As a result, two different signals could be distinguished (Fig. 5a); the first one, with hfs's $a_N = 7.2$ G and $a_H = 4.0$ G (two protons) can be safely attributed to the 5,5-dimethyl-2-oxo-pyrroline-1-oxyl (DMPOX); the second one, with hfs's $a_N = 13.6$ G and $a_H = 10.9$ G and 1.5 G corresponds to DMPO-SO_4, acting as an evidence for the formation of $SO_4^{\bullet-}$ through Eq. (3). The formation of •OH via Eq. (4) were not detected. This result suggests that DMPO acts as an electron donor for the one-electron reduction of PMS, preferentially resulting in the formation of $SO_4^{\bullet-}$ rather than •OH, with the simultaneous formation of DMPOX:

$$HSO_5^- + e^- \rightarrow OH^- + SO_4^{\bullet-} \quad (3)$$

$$HSO_5^- + e^- \rightarrow \bullet OH + SO_4^{2-} \quad (4)$$

Accordingly, PMS is expected to easily attack oxidable biomolecules present in bacteria. EPR measurements were performed in the presence of deoxyguanosine (dG) (Morikawa et al., 2014), the most electron-rich and readily oxidized site in DNA, and Tyrosine (Tyr), one of the most easily oxidized amino acids present in the cell wall (Warren et al., 2012). When PMS was added to the aqueous media containing dG, the one-electron oxidation of dG occurred, resulting in the formation of $SO_4^{\bullet-}$, which was trapped as DMPO-SO_4 (Fig. 5b). Although the oxidized form of dG (dOG) should be generated, this compound could not be detected by EPR experiments. Nevertheless, DMPOX, which results from the residual oxidation of DMPO, was detected.

To further assess the oxidation of dG, the samples were analyzed by UPLC-MS (Fig. 6a). The peak detected at *m/z* 283.0913 corresponded unequivocally to the oxidized species, 8-oxo-7,8-dihydroguanosine (dOG), which is clear evidence for the oxidation of dG. Several studies have monitored dOG levels to determine the intracellular oxidative stress levels. The dOG is the most well-studied DNA lesion. Although the results revealed only modest mutations, it has been reported that *E. coli* responds to DNA damage via another *recA-lexA*-mediated pathway, resulting in programmed cell death (Erental et al., 2014). Although the EPR spectra did not show the formation of DMPO—OH, dOG could have resulted not only from electron transfer oxidation but also from •OH radical addition. To further confirm or eliminate the involvement of •OH in dG oxidation, we monitored the formation of fluorescent 7-hydroxycoumarin from coumarin upon excitation at 330 nm (Fig. 6c) (Leandri et al., 2019). The absence of any enhancement in coumarin emission at 455 nm in the presence of dG and PMS revealed that fluorescent 7-hydroxycoumarin was not formed, which was in agreement with the lack of •OH radicals in the primary oxidation of dG.

Next, we studied the oxidation of Tyr-by PMS using EPR spectroscopy (Fig. 5c). In this case, the adduct DMPO-SO_4 was detected together with DMPOX, and less so with DMPO—OH. Under these reaction conditions, Tyr-acts as an electron donor, resulting in the formation of $SO_4^{\bullet-}$, which is trapped as DMPO-SO_4; the partial oxidation of DMPO results in the formation of DMPOX. However, the detection of DMPO—OH could have had two different origins, which may have resulted from the reaction (Eq. 3) or more likely due to the gradual decomposition of DMPO-SO_4 in water. Further confirmation of the oxidation of Tyr-was obtained from UPLC-MS analysis of their mixture, which revealed the unequivocal formation of the oxidized species 3,4-dihydroxy-L-phenylalanine (commonly known as DOPA) with an *m/z* of 197.0636, and dopachrome with an *m/z* of 193.9039 (Fig. 6b).

High bacterial inactivation was attained by PMS, as shown in Fig. 1, contrary to the lack of an effect produced by H_2O_2 or PDS, even though the oxidation potential described for PMS is ca. 1.82 V, whereas for PDS and H_2O_2, the potentials are ca. 2.01 V and 1.78 V, respectively. To elucidate this aspect, UPLC-UV experiments were performed to evaluate the reactivity between PMS, PDS, and H_2O_2 and several biomolecules, such as Tyr-and dG. The studies revealed oxidative reactions between these biomolecules and PMS or H_2O_2 but not in the presence of PDS (see Fig. S3). In the presence of PMS, complete conversion of Tyr-occurred after 90 min, with the concomitant formation of a yellowish product. In contrast, Tyr-levels remained unaltered after 90 min in the presence of PDS (Fig. S4b). Analogously, the oxidation of dG by PMS, PDS, or H_2O_2 was monitored by UPLC. Oxidation of dG by PMS or H_2O_2 also occurred, whereas dG remained unaltered in the presence of PDS for the same reaction times (data not shown). In conclusion, these results can be used as proxies of extracellular and intracellular damage.

Moreover, the oxidation of more complex biomolecules was explored to investigate the behavior of unactivated PMS by ^1H NMR. As electronegative groups move the ^1H NMR signals downfield, the presence of new peaks at approximately 8–9 ppm is associated with the presence of

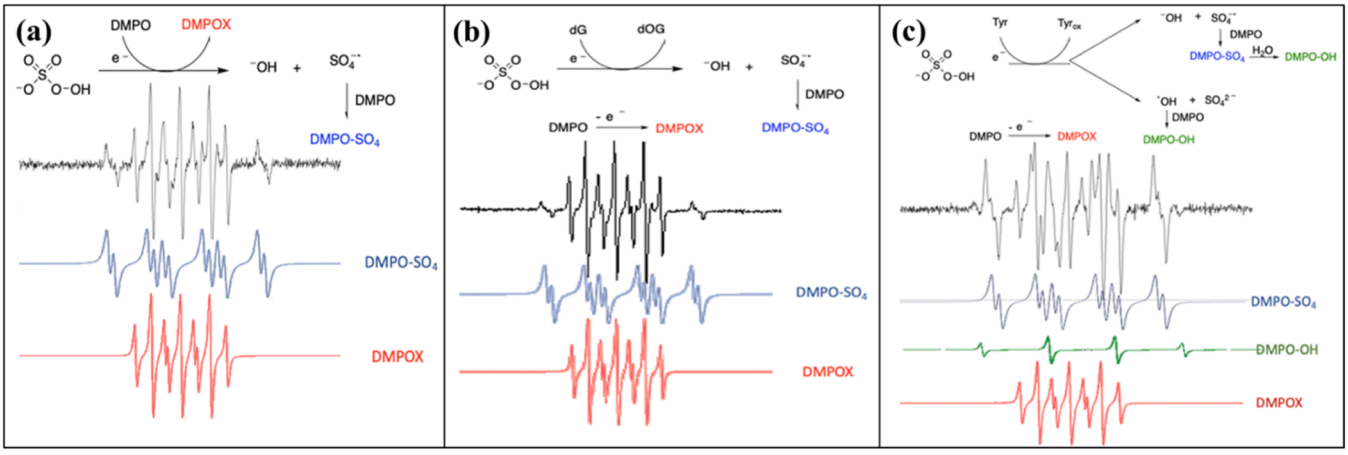

Fig. 5. EPR spectra of different systems: (a) PMS alone, (b) PMS and dG, and (c) PMS and Tyr. The black line represents the actual spectrum, and the blue, red, and green lines correspond to the deconvoluted spectra.

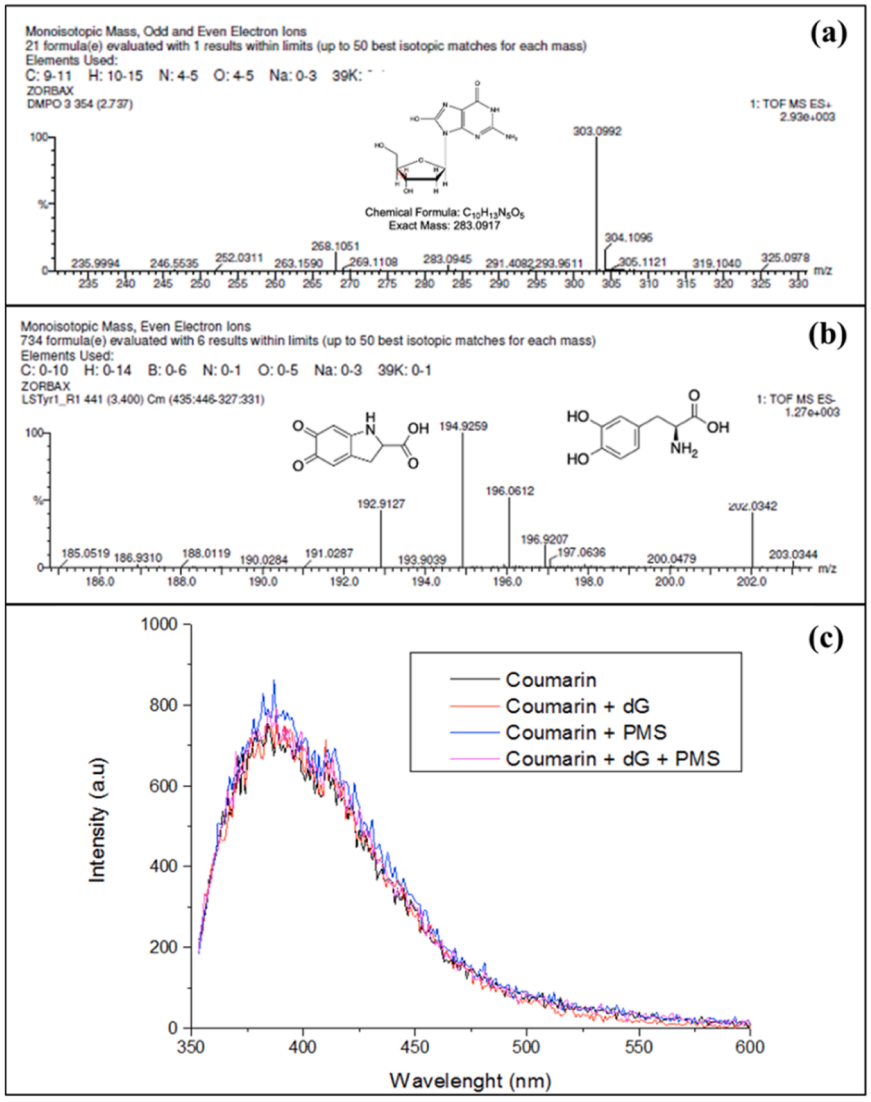

Fig. 6. (a) UPLC-MS detection of dOG in the PMS + dG reaction. (b) UPLC-MS detection of DOPA and dopachrome in the PMS + Tyr-reaction. (c) Emission spectra obtained upon excitation at 330 nm.

more electronegative atoms after the reaction with PMS, which changes the structure of the outer membrane of *E. coli* (Fig. S4a). In contrast, the LPS levels remained unaltered after PDS treatment (Fig. S4b). Thus, it has been clearly demonstrated that the activation of PMS is initiated by its redox reaction with the target biomolecules of bacteria, which, in addition to producing the oxidation of these biomolecules, generates the highly oxidative $SO_4^{\bullet-}$ (Eq. (5)). The as-generated $SO_4^{\bullet-}$ can further react with biomolecules (Eq. (6)). In addition, the initial electron transfer oxidation was followed by a reaction with molecular oxygen in a typical chain-triggered manner (Eq. 7).

$$HSO_5^- + \text{Biomolecule} \rightarrow OH^- + SO_4^{\bullet-} + \text{Biomolecule}^{\bullet+} \quad (5)$$

$$SO_4^{\bullet-} + \text{Biomolecule} \rightarrow SO_4^{2-} + \text{Biomolecule}^{\bullet+} \quad (6)$$

$$\text{Biomolecule}^{\bullet+} + O_2 + H_2O \rightarrow \text{Biomolecule-O-O}^{\cdot} + H_3O^+ \quad (7)$$

Moreover, the insignificant reactivity observed for PDS could explain its low bacterial inactivation. Although H_2O_2 shows similar reactivity to biomolecules as PMS, the ability of bacteria to scavenge ROS could explain the low bacterial inactivation observed. Thus, while effective bacterial inactivation occurs with PMS (0.1 mM), the minimum concentration of H_2O_2 required to inhibit bacteria is 1 mM (Rodriguez-Rojas et al., 2020).

3.5. *What is the Achilles heel of the bacterial cytoplasm? Investigation of intracellular effects via gene-knockout mutants*

3.5.1. *Contribution of ROS scavengers, defense regulators, iron sequesters, and genome repair enzymes*

The reactive species generated by the application of AOPs can destroy integral bacterial components and result in their inactivation via extracellular (short-lived species) and intracellular pathways (more stable species such as H_2O_2). Generally, the cytoplasm is considered to be an intracellular target site that includes DNA, RNA, enzymes, proteins, and ribosomes (Dutta et al., 2019). To elucidate intracellular PMS-mediated inactivation pathways, several *E. coli* mutants were used to identify the targets of intracellular damage caused by the knockout of specific genes. Hence, the wild-type (WT) strain and the corresponding single- and multiple-knockout mutants in their stationary phase were chosen.

First, the inactivation kinetics of the WT were compared with those of the knockout mutants of the genes responsible for expressing antioxidant defenses (catalases, KAT, and superoxide dismutases, SOD) and DNA repair (Fig. 7). The KAT^- mutant (double $katG^-$ $katE^-$ mutant) lacks genes encoding primary cell defenses against H_2O_2 stress, whereas the SOD^- mutant (double $sodA^-$ $sodB^-$ mutant) lacks both manganese-

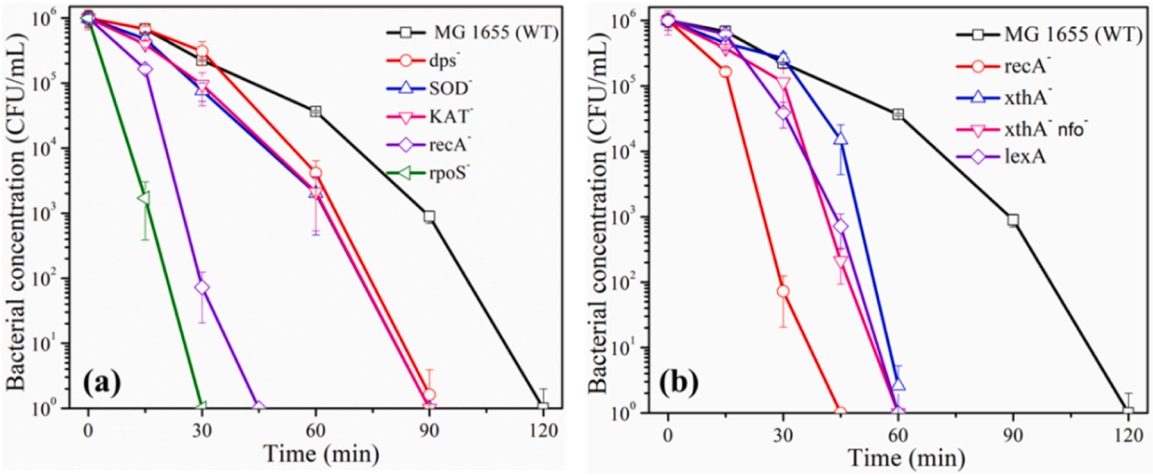

Fig. 7. Inactivation curves of WT *E. coli* and its derivative mutants by unactivated PMS. (a) MG 1655 and dps$^-$, SOD$^-$, KAT$^-$, recA$^-$, and rpoS$^-$ mutants and (b) MG 1655 and recA$^-$, xthA$^-$, double xthA$^-$nfo$^-$, and lexA mutants. Experimental conditions: [*E. coli*] = 10^6 CFU/mL (OD_{600}=0.005), $[PMS]_0$ = 30 mg/L.

and iron-co-factored superoxide dismutases, which can facilitate the dismutation of superoxide radicals into H_2O_2. As shown in Fig. 7a, 30 mg/L PMS led to the inactivation of 6-logU wild-type parent strain MG 1655 within 120 min. A similar trend was observed in the inactivation efficiencies of the two mutants (both SOD$^-$and KAT$^-$), suggesting that oxidative stress mediated by intracellular superoxide or H_2O_2 formation had either a moderate effect on bacterial inactivation in PMS treatment or the generation of superoxide and H_2O_2, respectively, occurred to a limited extent.

Furthermore, there was little sensitivity towards bacterial death from an iron-related mutant (*dps*$^-$); the *dps*$^-$ mutant lacks a mini-ferritin that sequesters iron during H_2O_2 stress (Mancini and Imlay, 2015). The low sensitivity of the *dps*$^-$ mutant revealed a low participation of PMS in intracellular activation by iron, contrary to the events taking place following the diffusion of H_2O_2 in the cell. However, both *the recA*$^-$ and *rpoS*$^-$ strains were inactivated more quickly than the WT parent strain. *RecA* mediates the DNA repair pathway. Its sensitivity indicates that a one-electron oxidation process occurs with DNA as its target, similar to Fenton-or •OH-mediated damage (Giannakis et al., 2022). Hence, PMS may generate either •OH or, according to the EPR results, $SO_4^{\bullet-}$ inside the cell, leading to cell death. The *rpoS*$^-$ mutant strain serves as a validation for almost all of the aforementioned pathways; this operon controls the induction of Dps, as well as antioxidant proteins. Considering the entirety of the results shown in Fig. 7a, the damage caused by PMS is not Fenton-like but rather a reaction of $SO_4^{\bullet-}$ with DNA or other cytoplasmic components.

According to the results of the *recA*$^-$mutant, DNA damage led to inactivation of *E. coli.* This corroborates the EPR findings with dG oxidation as a proxy. Hence, using these results as stepping stones, other derivative mutants with altered DNA repair capacity were tested for their sensitivity. As shown in Fig. 7b, *the xthA*$^-$, *xthA*$^-$ *nfo*$^-$, and *lexA* mutants were sensitive and rapidly inactivated within 60 min (less than that of the WT, 120 min). The *xthA*$^-$ strain lacks exonuclease III, which is the major apurinic/apyrimidinic (AP) endonuclease under normal growth conditions, whereas the *xthA*$^-$ *nfo*$^-$ strain lacks exonuclease III and endonuclease IV, two enzymes that complete the repair of oxidized DNA bases and frank strand breaks. *LexA* represses the transcription of several genes involved in the cellular response to DNA damage, inhibition of DNA replication, and DNA synthesis (Brent and Ptashne, 1980; Hu et al., 2017). In a similar test, but with H_2O_2 instead of PMS, *lexA* and various of its target genes were found upregulated after 10 min of exposure to 2.5 mM H_2O_2 in comparison with controls, suggesting a role for LexA in the H_2O_2 response (Roth et al., 2022). As such, two-electron oxidation, similar to that induced by H_2O_2, is also possible; the sensitivity of these mutants is lower than that of *recA*$^-$ but is important to its viability.

In the final validation step, experiments at 10^8 CFU/mL allowed better monitoring of PMS via its reaction with *E. coli* and its apparent reduction. Indeed, the parent strain presented a 4.2-logU decrease with 6.63 mg/L PMS consumption, whereas the *recA*- mutant showed an 11.31 mg/L PMS reduction (Fig. 8a). We hypothesize that since PMS can react more freely with intracellular components, a higher gradient with the bulk is generated, which causes a higher influx towards the cell, enhancing the inactivation and consumption of PMS. In contrast, experiments with exponential phase (growing) cells (Fig. 8b), which lack KatE and do not yet express Dps, showed that KatG was responsible for conferring (small) resistance to PMS, as it was not sensitive and that Dps had a moderate contribution. *RecA*$^-$ remained the most sensitive strain, but the SOD$^-$ mutant showed equally high sensitivity, possibly because of the higher loose iron content encountered in growing cells (vs. stationary phase) or Fe^{2+} leaching from Fe/S clusters. Hence, PMS activation inside the cells is possible, leading to faster cell death.

3.5.2. *Extent of DNA damage in healthy E. coli cells*

Because the DNA repair mutants were sensitive to PMS and dG was previously found to be degraded, we assessed the extent of intracellular damage. 16S rRNA was selected as a proxy for DNA damage in *E. coli*, and the average concentration of the 16S rRNA gene (copies/mL) during PMS exposure experiments carried out in the dark with two concentrations of PMS (30 mg/L and 50 mg/L) is shown in Fig. S5. The results did not reveal a high reduction in the number of copies of the 16S rRNA gene at either PMS concentration tested. An instantaneous 50 % decrease in 16S rRNA concentration from 2.3 × 10^8 copies/mL was observed when PMS was added (t = 0) reaching $1.07\times10^8\pm3.35\times10^7$ and $1.54\times10^8\pm5.38\times10^7$ copies/mL, for 30 and 50 mg/L PMS concentrations, respectively. However, after this time point, the number of gene copies remained stable throughout the experiment (Table 1). Most likely, the presence of DNA repair enzymes, active in healthy (WT) *E. coli* cells, repair the damage inflicted.

The results of this study indicated cell wall damage, protein oxidation, and DNA damage, but the gene quantification analyses showed a moderate effect, which can be attributed to the low PMS concentration assayed as well as the cell repair mechanisms, antioxidant defenses, and size of the 16S rRNA gene (i.e., detecting a longer sequence allows more attacks). Nevertheless, the immediate and significant decrease in gene copies, especially the quasi-stable number of copies, indicates that there is indeed damage to the cell; however, repair mechanisms can mitigate this damage. In addition, this may indicate that apart from extracellular events, intracellular targets other than DNA can lead to bacterial inactivation.

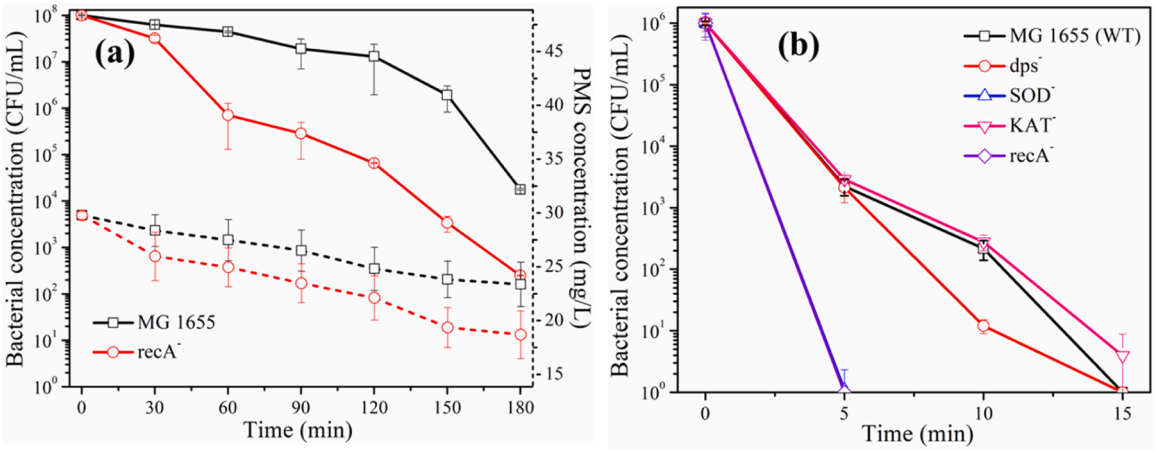

Fig. 8. (a) Inactivation curves of WT *E. coli* and the derived recA^{-} mutant by unactivated PMS and residual PMS concentration, (b) inactivation of WT *E. coli* and its derivative mutants in the exponential phase by unactivated PMS.

Table 1
Average and standard derivation of 16S rRNA quantification in a water matrix containing *E. coli* 498 at different concentrations of peroxymonosulfate (PMS).

Gene quantification with 16S rRNA copies/mL measurement, expressed in average ± standard deviation (SD)		
Time (min)	PMS concentration	
	30 mg/L	50 mg/L
Water + *E. coli*	$2.33\times10^{8}\pm2.15\times10^{7}$	$2.34\times10^{8}\pm1.04\times10^{7}$
0	$1.07\times10^{8}\pm3.35\times10^{7}$	$1.54\times10^{8}\pm5.38\times10^{7}$
60	$1.14\times10^{8}\pm1.80\times10^{6}$	$1.40\times10^{8}\pm2.12\times10^{7}$
120	$1.07\times10^{8}\pm4.45\times10^{6}$	$1.33\times10^{8}\pm7.09\times10^{7}$
180	$1.01\times10^{8}\pm1.58\times10^{6}$	$1.50\times10^{8}\pm8.78\times10^{7}$

3.6. Integrated proposition for the inactivation of E. coli by PMS

Based on a thorough evaluation of the above results and bridging the partial conclusions of each section, a proposition for an integrated, time-resolved mechanism for *E. coli* inactivation via PMS oxidation is shown in Fig. 9. The time points (in minutes) mentioned are relative, only to show the order of events and not precise kinetics. First, a steady reduction in *E. coli* (DSM498) cultivability was found, which corroborates the XTT assay results of declining metabolic activity and the indication of a dominant extracellular pathway. Early MDA detection (peak at only 5 min) confirmed the proposed extracellular oxidation, which is the result of an initial oxidation of Tyr-or other electron donor biomolecules through electron transfer reactions with unactivated PMS, in agreement with previous findings (Berruti et al., 2022), with the subsequent generation of highly reactive $SO_4^{\bullet-}$ and, to a lesser extent, •OH, $^1O_2$, and $O_2^{\bullet-}$, which was suggested as a possibility from the

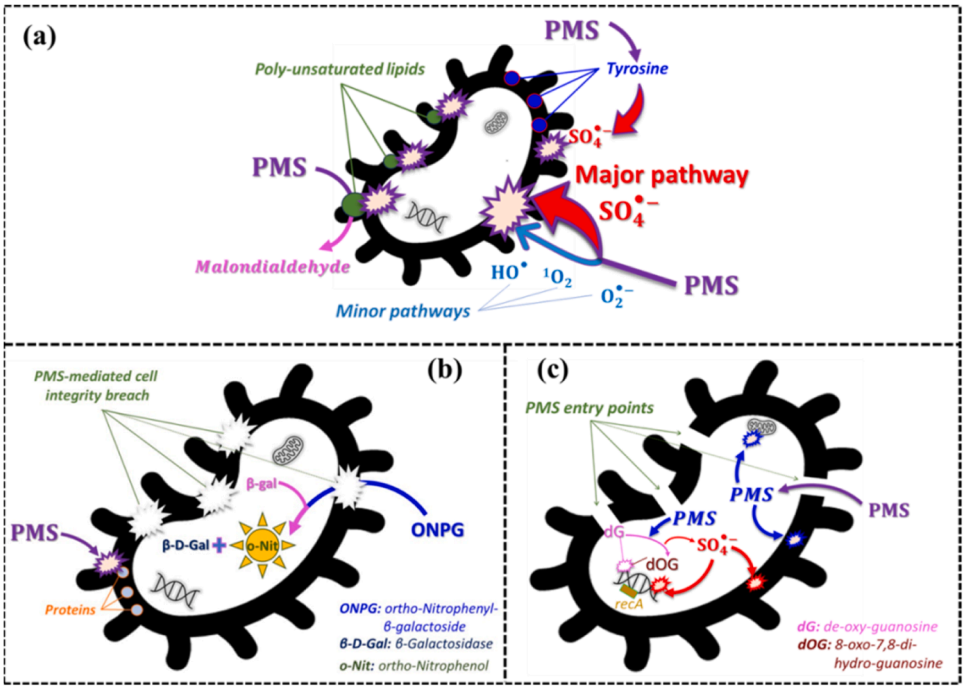

Fig. 9. Time-resolved integrated mechanistic pathway for *E. coli* inactivation. (a) Initial steps: lipid peroxidation via dominant and secondary pathways, with MDA as an indicator of oxidation. (b) Damage propagation: cell envelope disruption and protein oxidation with ONPG hydrolysis as an indicator of cell continuity loss. (c) Intracellular damage: cytoplasmic components and DNA damage with prevalent repair mechanisms.

scavenger tests performed. This damage leads to the loss of cell wall continuity, as demonstrated by the ONPG assay, with the maximum damage appearing at 30 min. The oxidation targets were mainly lipids and not proteins, as the Bradford assay showed low degradation, whereas the lipid peroxidation assay (MDA) and ^{1}H NMR with LPS isolated from *E. coli* (O111:B4) clearly indicated that LPS formed a prominent target. It is noteworthy that at 30 min, only 90 % of the bacteria lost their cultivability, and the XTT assay showed that 80 % of the cells could maintain a certain level of viability for as long as the cell integrity allowed for the assessment of intracellular oxidation events. Proteins were either not the main target or were harder to degrade; however, our experimental proof was restricted to Tyr.

Nevertheless, the oxidation of dG by $SO_4^{\bullet-}$ indicates that the reaction and DNA degradation are possible. The qPCR results showed low 16S rRNA gene copy reduction, which initially seems to have a low effect; however, considering that the cells dispose of an arsenal of defenses, the interpretation differs. In principle, PMS diffuses or penetrates the cell through continuity breaches, with the latter being more prominent as WT *E. coli* strains (MG 1655) show a shoulder in their inactivation. Although a peroxide, the PMS inside the cell, is not managed as H_2O_2 with catalases or dismutases and has a mild cytoplasmic oxidation effect via a Fenton-like reaction, the damage is centered at the DNA, but the possibility of affecting other components cannot be excluded. Here, it is important to note that there are various DNA repair mechanisms controlled by *recA, xthA, nfo*, and *lexA*, and all have a contribution; by using gene knockout mutants, we found that RecA is the most crucial protein. The type of intracellular damage revealed one-electron oxidation damage to the genome (dG is the most oxidizable target), and the other studied DNA repair mechanisms confer only a complementary effect. This explains the low degradation observed by qPCR, possibly because DNA repair occurs simultaneously or faster than the damage. Nevertheless, the panorama of actions shows an integral, multilevel bactericidal action, which explains the high efficacy of PMS.

4. Conclusions

The present study aimed to elucidate the effects of peroxymonosulfate on bacteria. The results showed that by adding equimolar concentrations of inorganic peroxides, PMS outperformed the others (H_2O_2 and PDS). Despite its lower oxidation potential, it can react with target biomolecules to generate the highly oxidizing reactive species $SO_4^{\bullet-}$, leading to radical reactions and cell death. Hence, if one considers only the chemistry of inorganic peroxides as disinfectants, PMS would be a very effective compound. Nevertheless, other parameters, such as cost, would affect the final choice of disinfectant. It should be noted that the final choice may change if, rather than the unaltered PMS, homolysis of the peroxide occurs to generate radicals, or if aspects such as cost, engineering, and the life cycle of oxidants are considered.

Furthermore, external oxidation leads to cell envelope disruption and intracellular oxidation, as shown by XTT, MDA, and ONPG analyses, and EPR and ^{1}H NMR measurements. However, despite their confidence, our results are not unequivocally true, since other Gram-negative bacteria may present slight differences in external or internal targets, as well as defense/repair mechanisms. In addition, Gram-positive bacteria have a very different cell wall composition and relative order of events. What is certain is that PMS will start the oxidation from the outside, which is a damage that has no repair mechanism.

Overall, this study reveals the substantial reactivity of PMS in the development of bacterial oxidative processes. Moreover, it is the view of the authors that this work, despite its apparent limitations, brings a new understanding of PMS-mediated disinfection, which is a very popular oxidant used in AOPs. The tests performed are crucial for explaining the baseline damage to *E. coli* in AOPs; consequently, these tests should be performed as blank controls prior to experimenting with PMS activation using energy or catalysts. These are exactly the tests whose effects are often overlooked or misinterpreted, and our results will assist researchers in setting the basis for further experimentation.

CRediT authorship contribution statement

Na Tian: Formal analysis, Investigation, Methodology, Writing – original draft, Writing – review & editing. **Luciana Carina Schmidt:** Formal analysis, Investigation. **María Jesús Abeledo Lameiro:** Methodology. **María Inmaculada Polo-López:** Investigation, Methodology, Writing – original draft. **María Luisa Marín:** Investigation, Methodology. **Francisco Boscá:** Formal analysis, Investigation, Methodology, Writing – original draft. **Isabel del Castillo González:** Supervision. **Aurelio Hernández Lehmann:** Formal analysis, Resources, Supervision. **Stefanos Giannakis:** Formal analysis, Funding acquisition, Supervision, Writing – review & editing.

Declaration of competing interest

The authors declare that they have no known competing financial interests or personal relationships that could have appeared to influence the work reported in this paper.

Data availability

Data will be made available on request.

Acknowledgments

This work was supported by the National Natural Science Foundation of China (Grant No. 42107102), the China Postdoctoral Science Foundation (No. 2020M672442), and the China Scholarship Council (CSC No. 202006415045). Stefanos Giannakis wish to thank the MCIN/AEI /10.13039/501100011033 and the European Union Next Generation-EU/PRTR for funding the DIGIT4WATER project "*Towards the Improvement of the Urban Water Cycle Resilience Through the Implementation of Digital Tools Based on Machine Learning Models and Water Reclamation Technologies*" (Reference: TED2021-129969A-C-32, and the DETRAS Project, "*Desinfección-Descontaminación de Efluentes Contra la Transmisión de la Resistencia en Antibióticos*" (Reference: APOYO-JOVENES-21-UXUKHL-88-WQWWQF), funded by the Comunidad de Madrid through the call "*Research Grants for Young Investigators from Universidad Politécnica de Madrid.*" María Luisa Marín and Francisco Boscá gratefully acknowledge the Universitat Politècnica de València, Ministerio de Universidades, and recovery plan Next Generation/EU for the financial support in the postdoctoral contract María Zambrano of Luciana Carina Schmidt, on behalf of the requalification of the Spanish University System (2021–2023). María Luisa Marín and Francisco Boscá would also like to acknowledge the Spanish Ministry of Science, Innovation, and Universities (TED2021-131952B-I00 and PID2019-110441RB-C33, financed by MCIN/AEI /10.13039/501100011033 and by the European Union Next Generation-EU/PRTR). María Jesús Abeledo Lameiro and María Inmaculada Polo-López wish to thank the Spanish Ministry of Science and Innovation for funding the NAVIA Project (References: PID2019-110441RB-C32 and PID2019-110441RB-C33, financed by MCIN/AEI/10.13039/501100011033).

Supplementary materials

Supplementary material associated with this article can be found, in the online version, at doi:10.1016/j.watres.2024.121441.

References

Amiri, Z., Moussavi, G., Mohammadi, S., Giannakis, S., 2021. Development of a VUV-UVC/peroxymonosulfate, continuous-flow advanced oxidation process for surface water disinfection and natural organic matter elimination: application and mechanistic aspects. J. Hazard. Mater. 408, 124634.

Berruti, I., Inmaculada Polo-López, M., Oller, I., Flores, J., Luisa Marin, M., Bosca, F., 2022. Sulfate radical anion: laser flash photolysis study and application in water disinfection and decontamination. Appl. Catal. B: Environ. 315, 121519.
Berruti, I., Nahim-Granados, S., Abeledo-Lameiro, M.J., Oller, I., Polo-Lopez, M.I., 2021a. UV-C peroxymonosulfate activation for wastewater regeneration: simultaneous inactivation of pathogens and degradation of contaminants of emerging concern. Molecules. 26 (16), 4890.
Berruti, I., Nahim-Granados, S., Abeledo-Lameiro, M.J., Oller, I., Polo-Lopez, M.I., 2023. Peroxymonosulfate/Solar process for urban wastewater purification at a pilot plant scale: a techno-economic assessment. Sci. Total Environ. 881, 163407.
Berruti, I., Oller, I., Polo-Lopez, M.I., 2021b. Direct oxidation of peroxymonosulfate under natural solar radiation: accelerating the simultaneous removal of organic contaminants and pathogens from water. Chemosphere 279, 130555.
Bianco, A., Polo Lopez, M.I., Fernandez Ibanez, P., Brigante, M., Mailhot, G., 2017. Disinfection of water inoculated with Enterococcus faecalis using solar/Fe(III)EDDS-H_2O_2 or $S_2O_8^{2-}$ process. Water. Res. 118, 249–260.
Brasca, M., Morandi, S., Lodi, R., Tamburini, A., 2007. Redox potential to discriminate among species of lactic acid bacteria. J. Appl. Microbiol. 103 (5), 1516–1524.
Brent, R., Ptashne, M., 1980. The lexA gene product represses its own promoter. Proc. Natl. Acad. Sci. USA 77 (4), 1932–1936.
Chen, Y.D., Duan, X.G., Zhou, X., Wang, R.P., Wang, S.B., Ren, N.Q., Ho, S.-H., 2021. Advanced oxidation processes for water disinfection: features, mechanisms and prospects. Chem. Eng. J. 409, 128207.
Cho, M., Kim, J., Kim, J.Y., Yoon, J., Kim, J.H., 2010. Mechanisms of Escherichia coli inactivation by several disinfectants. Water. Res. 44 (11), 3410–3418.
Choi, Y., He, H., Dodd, M.C., Lee, Y., 2021. Degradation kinetics of antibiotic resistance gene mecA of methicillin-resistant staphylococcus aureus (MRSA) during water disinfection with chlorine, ozone, and ultraviolet light. Environ. Sci. Technol. 55 (4), 2541–2552.
Dutta, V., Singh, P., Shandilya, P., Sharma, S., Raizada, P., Saini, A.K., Gupta, V.K., Hosseini-Bandegharaei, A., Agarwal, S., Rahmani-Sani, A., 2019. Review on advances in photocatalytic water disinfection utilizing graphene and graphene derivatives-based nanocomposites. J. Environ. Chem. Eng. 7 (3), 103132.
Ellwood, M.M.N., 1982. Chromosomal locations of the genes for rRNA in Escherichia coli K-12. J. Bacteriol. 149 (2), 458–468.
Erental, A., Kalderon, Z., Saada, A., Smith, Y., Engelberg-Kulka, H., 2014. Apoptosis-like death, an extreme SOS response in Escherichia coli. mBio 5 (4) e01426-01414.
Feng, L., Peillex-Delphe, C., Lu, C., Wang, D., Giannakis, S., Pulgarin, C., 2020. Employing bacterial mutations for the elucidation of photo-Fenton disinfection: focus on the intracellular and extracellular inactivation mechanisms induced by UVA and H_2O_2. Water. Res. 182, 116049.
Geeraerd, A.H., Valdramidis, V.P., Van Impe, J.F., 2005. GInaFiT, a freeware tool to assess non-log-linear microbial survivor curves. Int. J. Food Microbiol. 102, 95–105.
Gelover, S., Gomez, L.A., Reyes, K., Teresa Leal, M., 2006. A practical demonstration of water disinfection using TiO_2 films and sunlight. Water. Res. 40 (17), 3274–3280.
Giannakis, S., 2019. A review of the concepts, recent advances and niche applications of the (photo) Fenton process, beyond water/wastewater treatment: surface functionalization, biomass treatment, combatting cancer and other medical uses. Appl. Catal. B: Environ. 248, 309–319.
Giannakis, S., Gupta, A., Pulgarin, C., Imlay, J., 2022. Identifying the mediators of intracellular E. coli inactivation under UVA light: the (photo) Fenton process and singlet oxygen. Water. Res. 221, 118740.
Giannakis, S., López, M.I.P., Spuhler, D., Pérez, J.A.S., Ibáñez, P.F., Pulgarin, C., 2016. Solar disinfection is an augmentable, in situ-generated photo-Fenton reaction—Part 2: a review of the applications for drinking water and wastewater disinfection. Appl. Catal. B: Environ. 198, 431–446.
Giannakis, S., Voumard, M., Rtimi, S., Pulgarin, C., 2018. Bacterial disinfection by the photo-Fenton process: extracellular oxidation or intracellular photo-catalysis? Appl. Catal. B: Environ. 227, 285–295.
Hu, J., Selby, C.P., Adar, S., Adebali, O., Sancar, A., 2017. Molecular mechanisms and genomic maps of DNA excision repair in Escherichia coli and humans. J. Biol. Chem. 292 (38), 15588–15597.
Huang, Z., Maness, P.-C., Blake, D.M., Wolfrum, E.J., Smolinski, S.L., Jacoby, W.A., 2000. Bactericidal mode of titanium dioxide photocatalysis. J. Photoch. Photobio. A 130, 163–170.
Jiang, Y., Wang, Z., Huang, J., Yan, F., Du, Y., He, C., Liu, Y., Yao, G., Lai, B., 2022. A singlet oxygen dominated process through photocatalysis of CuS-modified MIL-101(Fe) assisted by peroxymonosulfate for efficient water disinfection. Chem. Eng. J. 439, 135788.
Jiménez, I.d.l.O., Giannakis, S., Grandjean, D., Breider, F., Grunauer, G., Casas López, J. L., Sánchez Pérez, J.A., Pulgarin, C., 2020. Unfolding the action mode of light and homogeneous vs. heterogeneous photo-Fenton in bacteria disinfection and concurrent elimination of micropollutants in urban wastewater, mediated by iron oxides in Raceway Pond Reactors. Appl. Catal. B: Environ. 263, 118158.
Karbasi, M., Karimzadeh, F., Raeissi, K., Giannakis, S., Pulgarin, C., 2020. Improving visible light photocatalytic inactivation of E. coli by inducing highly efficient radical pathways through peroxymonosulfate activation using 3-D, surface-enhanced, reduced graphene oxide (rGO) aerogels. Chem. Eng. J. 396, 125189.
Kohantorabi, M., Giannakis, S., Gholami, M.R., Feng, L., Pulgarin, C., 2019. A systematic investigation on the bactericidal transient species generated by photo-sensitization of natural organic matter (NOM) during solar and photo-Fenton disinfection of surface waters. Appl. Catal. B: Environ. 244, 983–995.
Lanrewaju, A.A., Enitan-Folami, A.M., Sabiu, S., Swalaha, F.M., 2022. A review on disinfection methods for inactivation of waterborne viruses. Front. Microbiol. 13, 991856.
Leandri, V., Gardner, J.M., Jonsson, M., 2019. Coumarin as a Quantitative Probe for Hydroxyl Radical Formation in Heterogeneous Photocatalysis. J. Phys. Chem. C 123 (11), 6667–6674.
Lee, H.J., Kim, H.E., Kim, M.S., de Lannoy, C.F., Lee, C., 2020. Inactivation of bacterial planktonic cells and biofilms by Cu(II)-activated peroxymonosulfate in the presence of chloride ion. Chem. Eng. J. 380, 122468.
López-Vinent, N., Cruz-Alcalde, A., Moussavi, G., del Castillo Gonzalez, I., Hernandez Lehmann, A., Giménez, J., Giannakis, S., 2022. Improving ferrate disinfection and decontamination performance at neutral pH by activating peroxymonosulfate under solar light. Chem. Eng. J. 450, 137904.
Luo, H., Liu, C., Cheng, Y., Zeng, Y., He, D., Pan, X., 2021. Fe(III) greatly promotes peroxymonosulfate activation by WS_2 for efficient carbamazepine degradation and Escherichia coli disinfection. Sci. Total Environ. 787, 147724.
Mancini, S., Imlay, J.A., 2015. The induction of two biosynthetic enzymes helps Escherichia coli sustain heme synthesis and activate catalase during hydrogen peroxide stress. Mol. Microbiol. 96 (4), 744–763.
McGuigan, K.G., Conroy, R.M., Mosler, H.J., du Preez, M., Ubomba-Jaswa, E., Fernandez-Ibanez, P., 2012. Solar water disinfection (SODIS): a review from bench-top to roof-top. J. Hazard. Mater. 235-236, 29–46.
Mohammadi, S., Moussavi, G., Shekoohiyan, S., Marín, M.L., Boscá, F., Giannakis, S., 2021. A continuous-flow catalytic process with natural hematite-alginate beads for effective water decontamination and disinfection: peroxymonosulfate activation leading to dominant sulfate radical and minor non-radical pathways. Chem. Eng. J. 411, 127738.
Morikawa, M., Kino, K., Oyoshi, T., Suzuki, M., Kobayashi, T., Miyazawa, H., 2014. Analysis of guanine oxidation products in double-stranded DNA and proposed guanine oxidation pathways in single-stranded, double-stranded or quadruplex DNA. Biomolecules. 4 (1), 140–159.
Oktyabrskii, O.N., Smirnova, G.V., 2012. Redox potential changes in bacterial cultures under stress conditions. Microbiology (N. Y) 81 (2), 131–142.
Qi, W., Zhu, S., Shitu, A., Ye, Z., Liu, D., 2020. Low concentration peroxymonosulfate and UVA-LED combination for E. coli inactivation and wastewater disinfection from recirculating aquaculture systems. J. Water Process Eng. 36, 101362.
Ramirez-Castillo, F.Y., Loera-Muro, A., Jacques, M., Garneau, P., Avelar-Gonzalez, F.J., Harel, J., Guerrero-Barrera, A.L., 2015. Waterborne pathogens: detection methods and challenges. Pathogens. 4 (2), 307–334.
Rodríguez-Chueca, J., Barahona-García, E., Blanco-Gutiérrez, V., Isidoro-García, L., Dos santos-García, A.J., 2020. Magnetic $CoFe_2O_4$ ferrite for peroxymonosulfate activation for disinfection of wastewater. Chem. Eng. J. 398, 125606.
Rodríguez-Chueca, J., Giannakis, S., Marjanovic, M., Kohantorabi, M., Gholami, M.R., Grandjean, D., de Alencastro, L.F., Pulgarín, C., 2019. Solar-assisted bacterial disinfection and removal of contaminants of emerging concern by Fe^{2+}-activated HSO_5^- vs. $S_2O_8^{2-}$ in drinking water. Appl. Catal. B: Environ. 248, 62–72.
Rodríguez-Chueca, J., Moreira, S.I., Lucas, M.S., Fernandes, J.R., Tavares, P.B., Sampaio, A., Peres, J.A., 2017. Disinfection of simulated and real winery wastewater using sulphate radicals: peroxymonosulphate/transition metal/UV-A LED oxidation. J. Clean. Prod. 149, 805–817.
Rodriguez-Rojas, A., Kim, J.J., Johnston, P.R., Makarova, O., Eravci, M., Weise, C., Hengge, R., Rolff, J., 2020. Non-lethal exposure to H_2O_2 boosts bacterial survival and evolvability against oxidative stress. PLoS. Genet. 16 (3), 1008649.
Roth, M., Jaquet, V., Lemeille, S., Bonetti, E.J., Cambet, Y., Francois, P., Krause, K.H., 2022. Transcriptomic analysis of E. coli after exposure to a sublethal concentration of hydrogen peroxide revealed a coordinated up-regulation of the cysteine biosynthesis pathway. Antioxidants 11 (4), 655.
Ruales-Lonfat, C., Benítez, N., Sienkiewicz, A., Pulgarín, C., 2014. Deleterious effect of homogeneous and heterogeneous near-neutral photo-Fenton system on Escherichia coli. Comparison with photo-catalytic action of TiO_2 during cell envelope disruption. Appl. Catal. B: Environ. 160-161, 286–297.
Sawyer, D.T., Valentine, J.S., 1981. How Super Is Superoxide? Acc. Chem. Res. 14 (12), 393–400.
Simpson, K.L., Hayes, K.P., 1998. Drinking water disinfection by-products: an Australian perspective. Water. Res. 32 (5), 1522–1528.
Von Gunten, U., Driedger, A., Gallard, H., Salhi, E., 2001. By-products formation during drinking water disinfection: a tool to assess disinfection efficiency? Water. Res. 35 (8), 2095–2099.
Wang, J.L., Wang, S.Z., 2018. Activation of persulfate (PS) and peroxymonosulfate (PMS) and application for the degradation of emerging contaminants. Chem. Eng. J. 334, 1502–1517.
Warren, J.J., Winkler, J.R., Gray, H.B., 2012. Redox properties of tyrosine and related molecules. FEBS Lett. 586 (5), 596–602.
WHO, 2017. Guidelines for drinking-water quality, Fourth edition incorporating the first addendum ed.
Xiao, R., Liu, K., Bai, L., Minakata, D., Seo, Y., Kaya Göktaş, R., Dionysiou, D.D., Tang, C. J., Wei, Z., Spinney, R., 2019. Inactivation of pathogenic microorganisms by sulfate radical: present and future. Chem. Eng. J. 371, 222–232.
Yan, J., Peng, J., Lai, L., Ji, F., Zhang, Y., Lai, B., Chen, Q., Yao, G., Chen, X., Song, L., 2018. Activation $CuFe_2O_4$ by hydroxylamine for oxidation of antibiotic sulfamethoxazole. Environ. Sci. Technol. 52 (24), 14302–14310.
Yao, S., Hu, Y., Ye, J., Xie, J., Zhao, X., Liu, L., Lyu, S., Lin, K., Cui, C., 2022. Disinfection and mechanism of super-resistant Acinetobacter sp. and the plasmid-encoded antibiotic resistance gene bla_{NDM-1} by UV/peroxymonosulfate. Chem. Eng. J. 433, 133565.
Zeb, A., Ullah, F., 2016. A Simple Spectrophotometric Method for the Determination of Thiobarbituric Acid Reactive Substances in Fried Fast Foods. J. Anal. Methods Chem. 2016, 1–5.